



SEISMIC EVALUATION OF CRITICAL MECHANICAL AND PIPING COMPONENTS INSIDE A NUCLEAR POWER PLANT CONTAINMENT BUILDING

N. Ioannidis¹, A. Athanasiou¹, A. G. Sextos^{1,2} and G. D. Manolis¹

¹Department of Civil Engineering, Aristotle University of Thessaloniki, Greece

²Department of Civil Engineering, University of Bristol, UK

Abstract

This work focuses on the dynamic response of nuclear power plant mechanical sub-systems (i.e., main cooling system, steam generators, emergency cooling injection tanks and piping) that are housed within the containment structure and are associated with power generation. More specifically, the numerical modeling procedure focuses on the internal R/C wall structural system, which is used for supporting the mechanical equipment. Next, the complex grid of the mechanical components is modeled with shell finite elements. This internal equipment configuration is then excited by a suite of earthquake ground motions. Following extensive parametric studies, the seismic demand imposed on the internal equipment is assessed on the basis of the results from the dynamic stress analysis of the critical components. It is shown that, depending on frequency content of the incoming seismic motion, abrupt uplift that may take place, even for moderate intensity, particularly when the containment structure rests on soft soils. This situation may produce peaks in the pipe elbow strains that could potentially affect the serviceability, operation and under extreme conditions, the safety of the entire nuclear power plant, thus, they should be considered in the design process.

Keywords: nuclear power plants; containment structure; mechanical equipment; soil-structure-foundation interaction

1. Introduction

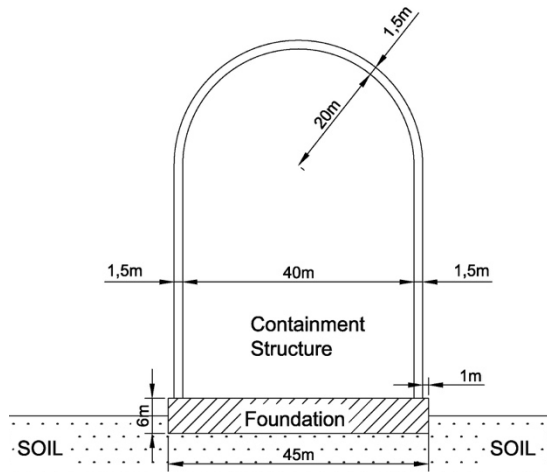
Nuclear power plants (NPP) are a reliable and efficient source of power in general and electricity in particular for modern, industrialized societies that pursue both economic growth and reduced CO₂ emissions [1]. There is, of course, much skepticism in the general public regarding the consequences of even a minor nuclear accident. For this reason, many precautionary measures are routinely taken and limit states are assessed in the design of the NPP containment structure (see ASCE 1998 [2]; ASCE, 2005 [3]). In this work, we study the response of internal sub-systems within a seismically excited NPP containment structure that are associated with power generation. More specifically, the safety systems that are critical for normal NPP operations, such as the main cooling system, the steam generators and the emergency cooling injection tanks along with the connecting piping network are all studied through numerical modeling by the finite element method (FEM), see [4].

In general, utility companies make every effort to build NPP on rock outcrop, or at least on firm soils. This is engineering common sense, given that NPP comprise heavy structures such as the containment building, so that foundation (uniform or differential) settlement is avoided under routine operating conditions while site amplification effects in seismically-prone regions are kept to a minimum [5]. Occasionally, it is not possible to abide by these guidelines, especially in heavily-populated countries and/or countries where the major urban centers are concentrated along the coastline [6,7]. For cases such as these, the presence of a heavy and stiff structure founded on soft soil triggers soil-structure-interaction (SSI) phenomena, both in terms of elongation of the fundamental period of the combined NPP- soil system and the characteristics of the Foundation Input Motion itself [8]. This is a problem of particular interest given the complex response of soft soils under strong earthquake ground motion, which as shown by the Fukushima event, may well exceed the design seismic actions. It is also noted that a new appendix has been added to the forthcoming edition of ASCE Standard 4 to provide guidance for time-domain, SSI analysis considering both material nonlinearity of the soil domain and geometrical nonlinearity (i.e., uplift and sliding) at the soil-foundation interface [9]. Along these lines, the scope of this paper is to scrutinize the effect of soft soil conditions on the dynamic response of the containment building and, at a second level, on the

serviceability and safety of its critical mechanical and piping components. For this purpose, a typical containment building is studied under a suite of well selected earthquake ground motions applied at the bedrock of a refined, three dimensional finite element (FE) model.

2. Overview of the NPP studied

A typical Westinghouse pressurized water reactor (PWR) containment structure is studied in this work, composed of a circular base slab, an upright cylinder as the main structure and a hemispherical dome, as shown in Fig. 1. The PWR has a height of 85.8m, wall thickness of 1.5m and is partially embedded in the supporting ground. The reinforcement of the containment is composed of $\varnothing 40$ mm bars at 80mm spacing, running both ways at the inner and outer faces of the cylindrical R/C wall, continuing within the spherical dome with an assumed effective concrete cover of 100mm [10]. Material properties are summarized in [11] as well as in the Table embedded in Fig. 1. Material properties are defined within the elastic region on the basis of the envisaged linear elastic response performance objective of the containment building. Given its excessive stiffness, the latter is further treated as a rigid body.



Concrete	
Compressive Strength f_c (MPa)	35
Tensile Strength f_t (MPa)	2
Modulus of Elasticity (GPa)	28
Poisson's Ratio	0.2
Strain at compressive strength	0.0035
Density (kg/m^3)	2500
Steel	
Modulus of Elasticity (GPa)	200
Yield Stress (MPa)	460
Density (kg/m^3)	7850

Fig. 1: Geometry and material characteristics of the containment building studied.

In order to numerically simulate the seismic behavior of the containment-foundation structural system, a nonlinear dynamic analysis is carried out using the Newmark-beta method. Two geological profiles are considered, namely stiff sand and competent rock, as being representative of the ground conditions in the Central and Eastern United States, respectively, see [12]. Both soil sites consist of a 100m deep, uniform (i.e., single layer) profile and rest on elastic, viscously damped bedrock. The shear wave velocity of the two studied soil profiles are taken equal to $V_s=300\text{m/s}$ (with unit weight of $\gamma=20.1 \text{ kN/m}^3$) and $V_s=2500\text{m/s}$ and unit weight of $\gamma=23.3 \text{ kN/m}^3$, for the sand and rock case, respectively. Particularly for the first case, an equivalently reduced, linear shear modulus is assumed for the purposes of site response analysis equal to $G=0.7G_0$ (i.e., 70% of its initial value) and an approximate means of considering soil nonlinearity under strong ground motion.

2.1 The internal structure

The internal structure of a typical pressurized water reactor (PWR) is composed of an R/C wall structure whose purpose is to support the mechanical components which are vital for the normal operation of the NPP. These components are primarily the nuclear reactor and the main cooling system, which comprises the steam generators and the circulation pumps, along with the piping system that interconnects them. The structural integrity of the cooling system is of paramount importance and must be maintained under all conditions. Thus, depending on the level of a possible cracking, problems in the circulation and the heat dissipation ability of the system may occur, particular under a loss-of-coolant accident (LOCA) event [13].



In order to assure the structural integrity of the cooling system, the main strategy proposed by the Boiler and Pressure Vessel Code (BPVC), see ASME 2010a [14] is to keep the nominal stress that develop in the system components under the allowable stress, which in turn depends on the material itself and the operating temperature as discussed in ASME 2010b [15]. The BPVC divides nominal stress into a primary and a secondary component, representing stresses from equilibrium forces and from displacement compatibility, respectively. The BPVC allows exceedance of the nominal stress for temporary actions such as earthquake, depending on the characterization of the piping. For instance, nuclear Class 1 piping nominal stress (S_n) must not exceed three times the allowable stress intensity (S_m), i.e.,

$$S_n < 3S_m \quad (1)$$

In this paper, the seismically-induced state of stress in the main cooling system piping network is evaluated by taking into account external SSI phenomena manifested in the NPP containment building, and more precisely on the geometrically nonlinear phenomena such as uplift, sliding and rocking across the soil-foundation interface. To this purpose, a detailed 3D FEM model of the internal structure is created, whereby both the internal R/C walls and the nuclear reactor with its main cooling system are modeled. Four different analysis approaches are comparatively examined, as discussed in Section 2.2 below.

2.2 Alternative NPP analysis approaches

The main goal of the numerical analyses presented herein is to make exploratory calculations for the seismically-induced state of stress in the mechanical equipment, to be used to compare the different modeling techniques. Apparently, these dynamic stresses must be combined with the other actions influencing the piping system such, as internal pressure or constrained thermal expansion for the determination of the final nominal stress according to ASME [14]. The purpose, however, is not to quantify the probability of exceeding a certain level of damage but rather to comparatively assess the degree that the modeling assumptions regarding the soil and the soil-foundation interface may increase in the induced stress in the internal mechanical and piping system. Along these lines, four different cases were considered for the soil-structure system illustrated in Fig. 2, as listed below:

Case A: Response Spectrum Analysis of the containment building assumed to be fully fixed (RSA, no SSI). Use is made of the Eurocode 8 design response spectrum [16] for soil type C, ground acceleration $a_g=0.36g$ and the minimum permissible behavior factor $q=1.5$.

Case B: Linear Response History Analysis of the NPP containment structure assuming rock supporting conditions (LRHA, no SSI). Thirty, three-component, ground motions are selected and used as input directly at the base of the building, hence, both kinematic and inertial SSI phenomena are neglected.

Case C: Equivalent-linear Response History Analysis of the NPP containment structure assuming soft soil supporting conditions (LRHA, plus SSI). Soil compliance and the subsequent effect on the dynamic characteristics of the soil-structure system is addressed, along with the modification of the bedrock motion due to the response of the overlying soil layer, which as already mentioned is considered with equivalent reduced shear modulus of $G=0.7G_0$. No uplift or sliding is taken into consideration across the soil-foundation interface.

Case D: Geometrically nonlinear, material equivalent-linear, Response History Analysis of the NPP containment structure assuming soft soil supporting conditions and geometrically nonlinear SSI effects (NLRHA, plus SSI). This time uplift, sliding and rocking are permitted to materialize along the soil-foundation interface.

It is noted that in cases B, C and D the same thirty ground motions are used at the bedrock of the FEM model, to account for identical hazard conditions.



3. NPP mechanical system: CAE and FEM model

The seismic analysis of the various NPP subsystems is usually conducted using the equivalent beam model [17,18] to represent their stiffness, with all mass lumped at a reduced number of degrees-of-freedom (DOF) as compared to their original number. This modeling procedure is broadly used as it produces a simple mechanical model that is efficient in representing the basic eigenmodes of the structure at an affordable computational cost. Along these lines, the seismic input for the secondary systems is implemented in terms of in-structure response spectra or in-structure time histories. This modeling procedure has its benefits, but also its limitations considering the difficulty in an accurate representation for the subsystems.

The development of easy to use 3D modeling tools and analysis software, such as the Abaqus CAE [19], along with advances in the solvers developed for parallel computing, is shaping new avenues in the analysis of complex engineering systems. In this section, a 3D computer-aided, blueprint-type model of the main mechanical components of the studied NPP pressurized water reactor (PWR) is created, using published information from the Atomic Energy Commission of Canada [20]. This 3D CAE model is then imported in the FEM software for generating the mesh, assigning the mechanical properties, and solving. Following this procedure, the FEM model produced is as complex as needed, apparently at a relevant computational cost. Multiple load cases, such as fluid-structure-interaction, constrained thermal expansion, etc., can be separately analyzed and are not studied herein.

The internal structure of the containment building is an R/C wall structural system that is 40m high, see Fig. 3(left). It is nearly circular in plan and supports the reactor, two steam generators, four circulation pumps and the connecting piping network, plus the emergency injection cooling tanks. This support structure is symmetrical about the Y-axis and nearly so about the X-axis. It has two distinct, tower-like structures that house and support the steam generators. The walls range from 1.5-3.0m thick in order to support the mechanical components, but also for radiation shielding purposes. As a consequence, this structural system is quite stiff despite its large dimensions and mass. The R/C walls are modeled using 3D solid, ten-node tetrahedral, second order finite elements (C3D10). The largest element edge length in the FEM mesh was set to 2.5m, getting progressively smaller, in order to follow the wall geometry. The FEM mesh was extended so as to model the mechanical components by using linear shell, four-node with reduced integration FE (S4R). An appropriately high value for the shell FE thickness was assigned so as to approximate the large stiffness in components such as the reactor, the steam generators and the circulation pumps. These components are anchored into the walls with connecting steel beams for operational safety reasons. Finally, the piping system represents a two stage mechanical system, with stage one comprising small piping networks that pass through the reactor, while stage two is for large diameter steel pipes that circulate the accumulated cooling water in the steam generators and the circulation pumps. The two piping stages are connected in the accumulator/distributor cylinders. In more detail, the second stage pipes are 0.6 m in diameter, while those of the first stage are 0.4 m in diameter. The wall thickness of the pipes, despite the fact that they have many bends, is calculated in accordance to the American Society of Mechanical Engineers [14] formula for a straight pipe, which is linked to the BPVC [15] code regulation for allowable stress in carbon steel SA-106, Grade B, and for an operational internal pressure of 10MPa that is linked to an operational temperature in the range 270°-300°C.

Concrete class was taken C30/35 without any reduction factors, since no cracking in the concrete is expected for that level of ground motion intensity in the containment building. Mechanical properties of the carbon steel parts in the mechanical components, are also listed in Table 1 below.

Table 1 – NPP internal mechanical system material properties

	Concrete	Steel	
Modulus of elasticity (E)	22.8	205.8	(GPa)
Poisson's ratio (ν)	0.2	0.3	
Density (ρ)	2500	8000	(Kg/m)

The mechanical components (see Fig. 3, right) were modeled with a linear shell four-node FE with reduced integration (S4R), and the mass of the water was added to the material mass density. The largest FE side for the mechanical components such as the reactor, the steam generators, the pumps and emergency injection cooling tanks, along with the steel beams that connect them with the R/C wall structure was 0.5m, and for piping Stages 2 and 1 equal to 0.4 m and 0.15 m, respectively. The mesh used here comprised approximately 80,000 FE overall, while the internal structure model required 104,000 nodal points, see Fig. 4. The FEM mesh transition from the mechanical elements modeled with shell FE to the R/C structural wall that is modeled with solid FE elements was realized by mesh densification at the interface of solid and shell elements, in order to create common connection nodes. The total mass of the internal structure is 30,000 tons, the R/C supporting structural system weighs about 27,700 tons, representing 92% of the total mass and the remaining 8% belongs to the mechanical components. It is noted that the ASCE 4-98 (ASCE, 2005) requires coupled analysis of the structural system with its internal secondary systems if the latter mass is over 1% of total.

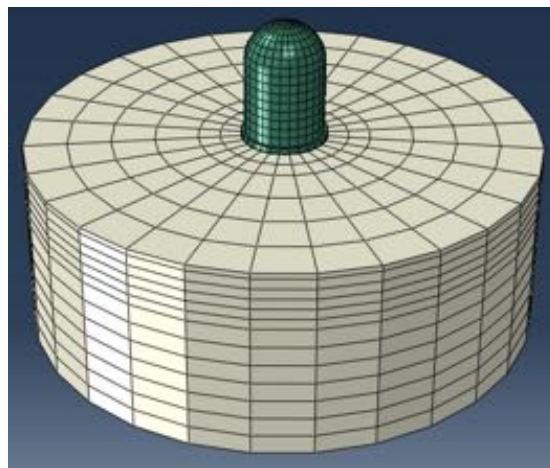


Fig. 2 – FEM mesh of NPP containment structure and supporting soil.

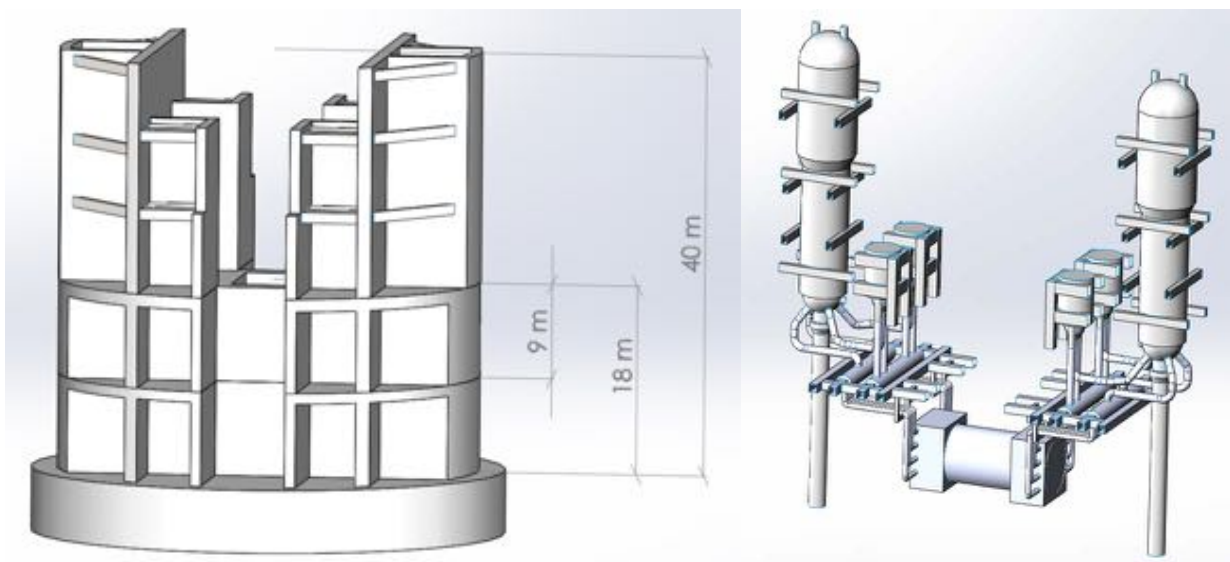


Fig. 3 – Isometric view of the wall support structure (left) and the main mechanical elements (right).

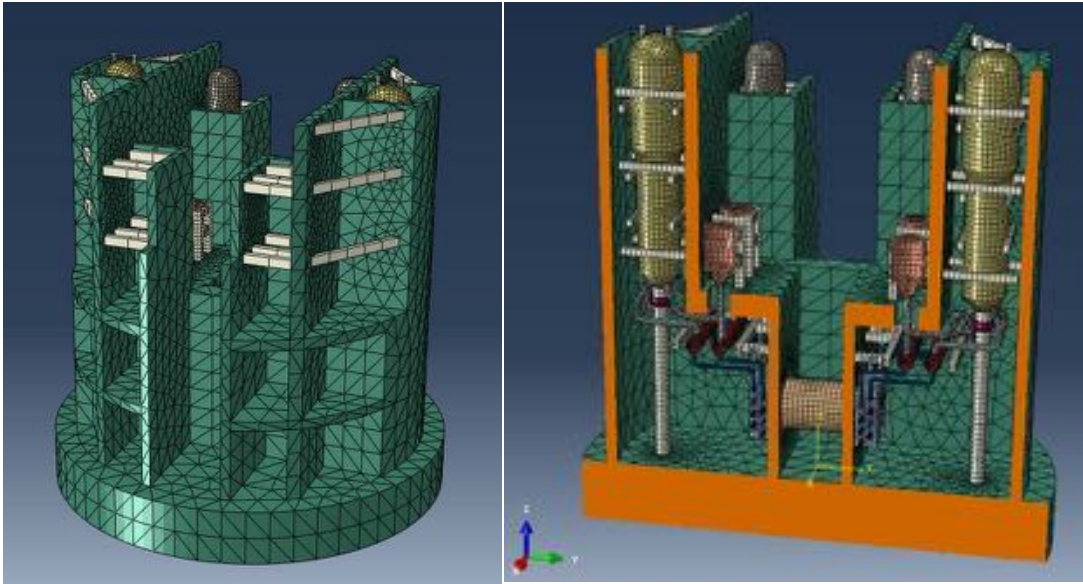


Fig. 4 – FEM meshing of the wall support structure (left) and the main mechanical elements (right).

4. Dynamic analysis of the NPP system

In order to calculate the transient response of the internal structure of the NPP containment building, a modal analysis was conducted first to determine the system natural modes and frequencies. More specifically, sixty eigenmodes were calculated by linear perturbation with Lanczos eigen-solver, for frequencies reaching up to 20 Hz. The first two modes calculated are presented in Fig. 5. Given that for an increase from 60 to 80 eigenmodes, the difference in response spectrum analysis estimates of the piping system was calculated to be less than 0.1%, hence, the total number of 60 eigenmodes was deemed sufficient for all further calculations involving the aforementioned four dynamic loading cases. In computing maxima in the dynamic stresses, the SRSS modal combination rule was used along with modal damping of 5%.

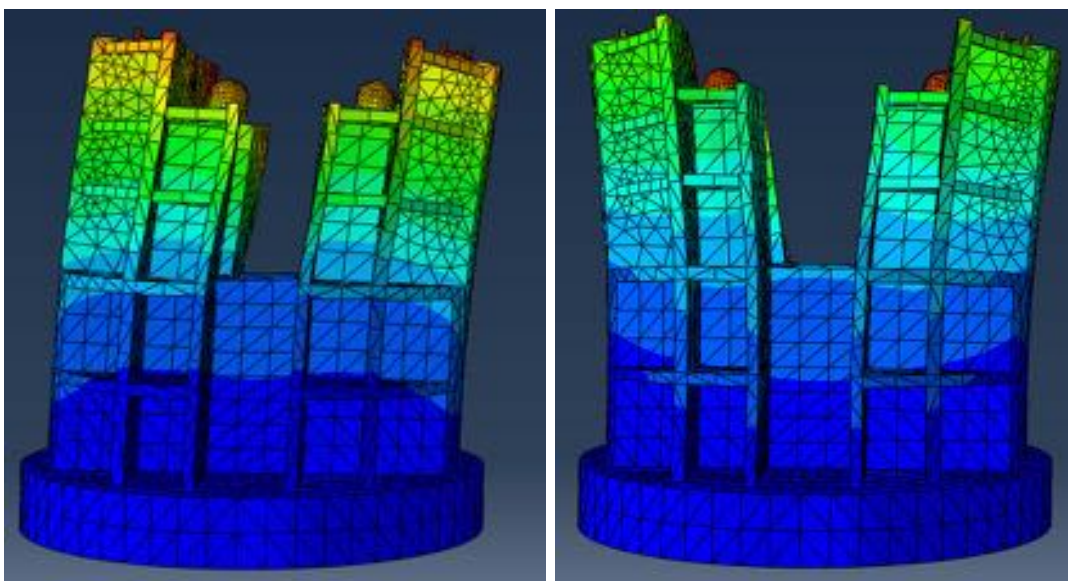


Fig. 5 – 1st internal NPP soil-structure mode at 5.23 Hz (left) and 2nd mode at 5.83 Hz (right).

4.1 Case A: Response Spectrum Analysis

A response spectrum analysis (RSA) was conducted in order to explore the behavior of the internal structure and its attached mechanical components acting as secondary systems. As already mentioned, the design Eurocode 8 spectrum was used for Soil type C, peak bedrock acceleration of $a_g=0.36g$, a behavior factor $q=1.5$, and for 5% modal damping ratio. The maximum spectral absolute displacement from the RSA is presented in Fig. 6. Given the high stiffness of the containment building it is computed of the order of 1cm in both X- and Y- directions, thus corresponding to a mere drift of 0.01%, which is of course an indicator of linear elastic response (and zero damage) under the design earthquake. Fig. 7 illustrates the maximum RSA displacements in a cross-section of the internal structure, where it is observed that the seismic demand is higher in long, unanchored pipe segments, as a result of the inherent flexibility of the piping system.

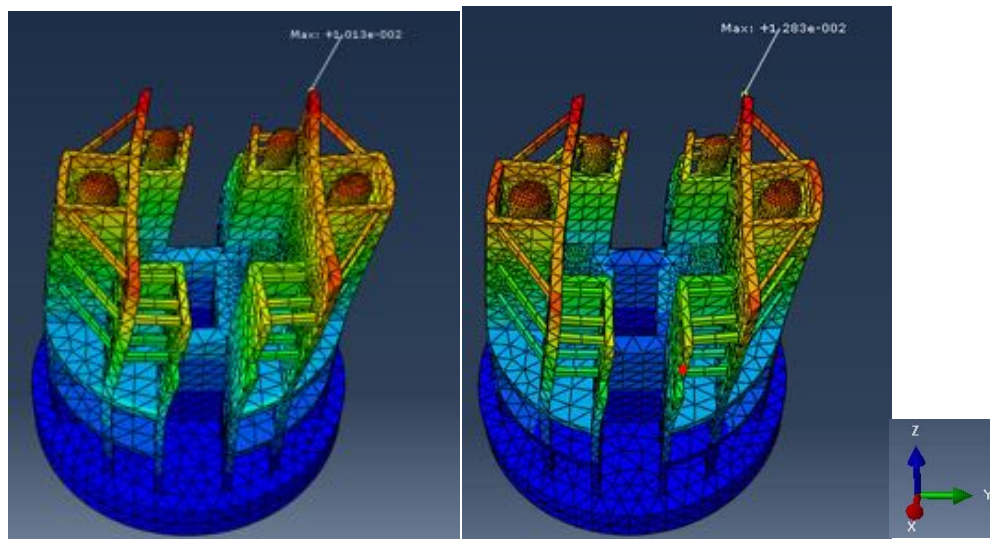


Fig. 6 – Maximum displacement for case A: Excitation in the X-direction (left) and Y-direction (right)

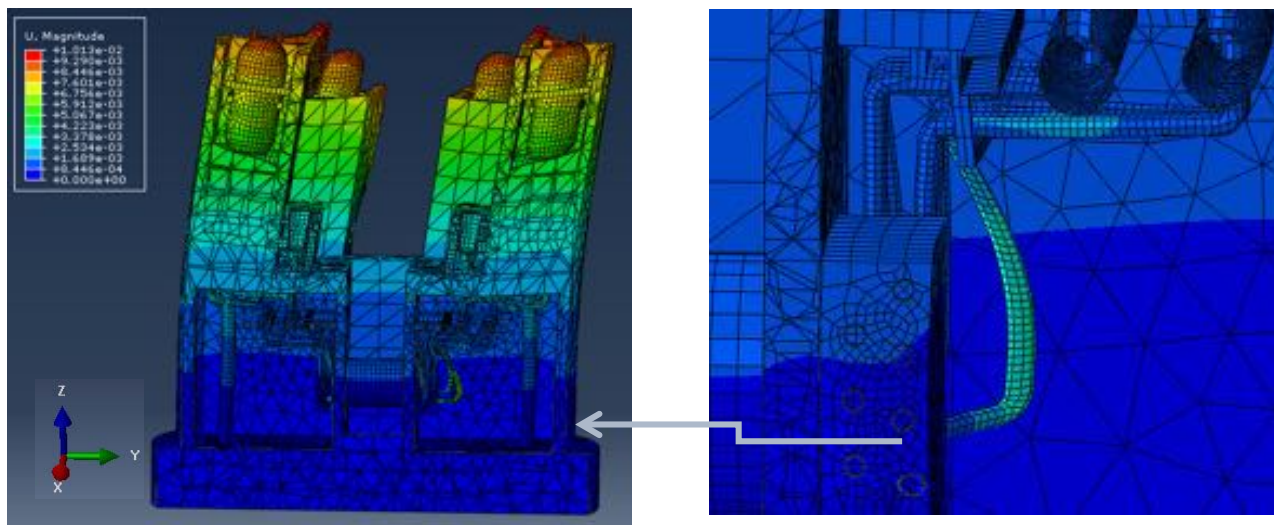


Fig. 7 – Maximum dynamic displacement distribution in the NPP internal structure as computed from the response spectrum analysis in the X-direction (left). Piping system detail (right).

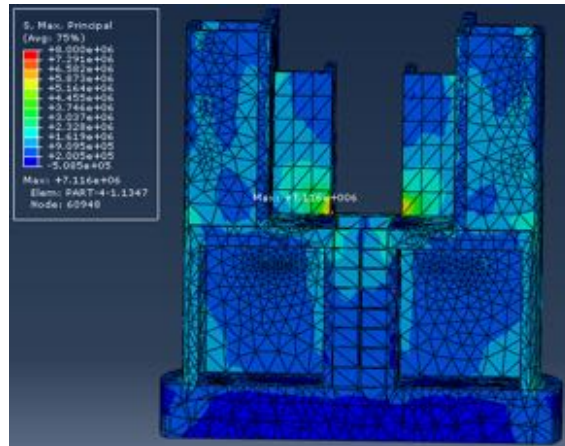


Fig. 8 – Maximum principal dynamic stress distribution in the NPP internal structure.

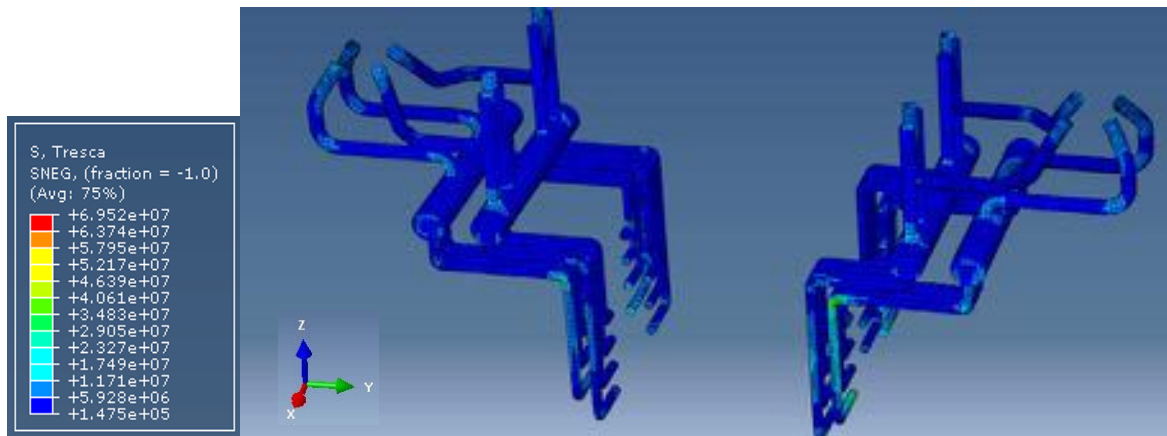


Fig. 9 – Tresca stress distribution in the piping system for excitation in the X-direction.

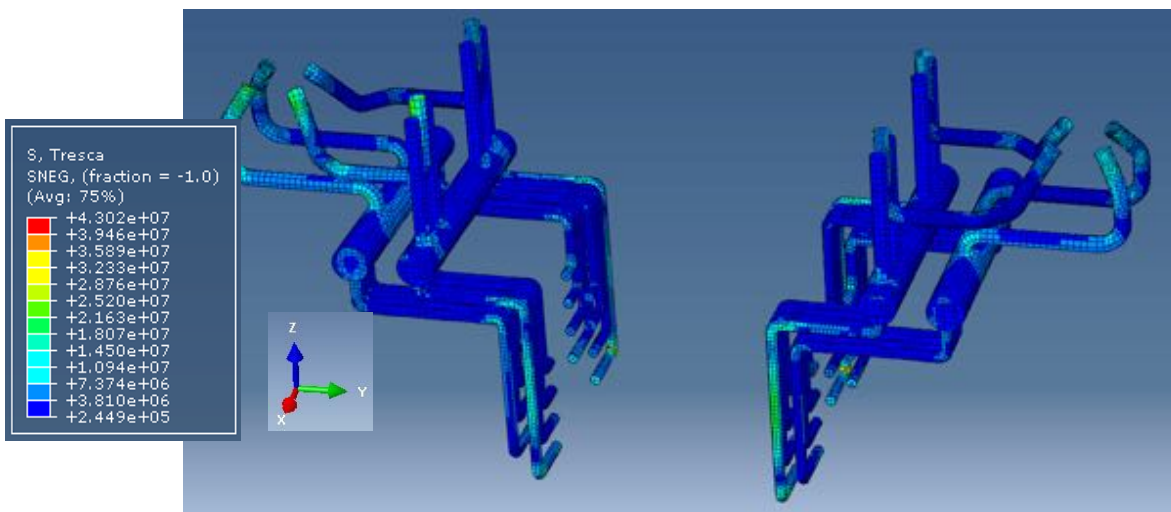


Fig. 10 – Tresca stress distribution in the piping system for excitation in the Y-direction.

As far as the principal dynamic stresses are concerned, Fig. 8 gives a general overview of their distribution within the internal structure, whereas, Figures 8 and 9, present Tresca stress distribution in the piping system for excitation in the X- and Y-direction, respectively [14,21]. It is observed that the seismically-induced stress is accumulated in the elbows and in the various connections with other mechanical components, while relatively small stress values register along the straight pipe sections. For instance, in Fig. 9 it is shown that along the straight pipe segments, stress values are in order of 0.5 to 1 MPa, as compared to values of 20-30 MPa that developed in the elbows.

4.2 Cases B-D: Response history analyses

All three Cases B, C and D use the extracted 60 modes of the internal structure as the basis to conduct modal response history integration. As previously mentioned, thirty recorded ground acceleration time histories are used for each case. In the Newmark-beta time integration algorithm, the time step used is 0.05s. The resulting maximum dynamic stress tensor from each time history record, along with the calculated maximum stress from the RSA of Case A, are presented in Tables 2-4 for ground motions of different frequency content (i.e., low, medium and high). It is observed that there are significant differences in the maximum response as registered by the different analysis approaches (i.e., with or without SSI and with or without soil-foundation contact effects). A first observation in all three Tables (suites of motions with different frequency content) is that on average, the Response Spectrum Analysis of the fixed-based system (Case A) leads to higher seismic demand, compared to the all Response History Analysis cases, despite the fact that the accelerograms were scaled accordingly so that their mean spectrum matched that of the design target one.

It is also evident that stresses from Case D, that even though stresses in the piping system are on average higher for excitation along the X direction, in terms of maxima, there is no critical X or Y direction as the seismic demand can be higher or lower for different excitation records and axis of excitation. Another interesting observation is that when geometrical nonlinearities in form of uplift and sliding in the soil-foundation interface are taken into consideration, the developed (average and maximum) stresses and generally 50-100% higher compared to Cases B and C neglecting this effect with the exception of high frequency ground motions. This effectively implies that the mechanical equipment of NPPs resting on soft soils and subjected to far-field, long period earthquake ground motions are susceptible to significantly increased seismic demand particularly at the piping elbows that may well exceed the design value by roughly 25-60% for the Y and X direction, respectively.

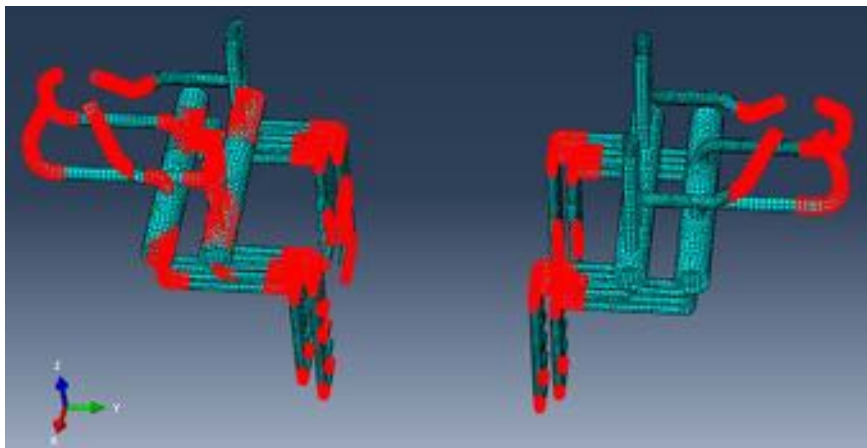


Fig. 11 – Critical regions in the piping system as computed from the time history stress analysis.



Table 2 – Maximum stress (in MPa) recorded in the piping system from the time history analyses: Low frequency excitations in both X- and Y- directions for all cases A-D

<i>Tm 3</i>	<i>NL</i>	<i>Case A</i>	<i>Case B</i>	<i>Case C</i>	<i>Case D</i>	<i>CaseA</i>	<i>CaseB</i>	<i>CaseC</i>	<i>CaseD</i>
					X Direction				
ChiChi	-		12,5	22,7	29,9		9,8	18,0	18,0
Coalinga	R-S		12,1	23,6	42,2		10,9	19,2	34,4
Imp Val EMO	S		12,9	19,0	20,3		9,8	15,7	17,6
Imp Val ECC	R-S		14,0	24,4	56,6		12,8	19,2	38,7
Imp Val BRA	-		19,5	20,4	16,8		14,5	14,0	14,5
Kobe	R-S	50,4	11,2	33,8	56,7	35,8	9,5	30,0	37,8
Kocaeli	R-S	(RSA)	12,9	29,6	79,5	(RSA)	11,7	26,0	43,1
Loma P	R-S		10,5	37,5	51,0		9,0	32,0	37,7
North	R-S		11,5	18,5	28,1		10,0	16,2	23,0
Smart	R-S		11,2	28,9	49,4		6,9	25,7	32,4
AVERAGE			12,8	25,8	43,1		10,5	21,6	29,7
MAX			19,5	37,5	79,5		14,5	32,0	43,1

Table 2 – Maximum stress (in MPa) recorded in the piping system from the time history analyses: Medium frequency excitations in both X- and Y- directions for all cases A-D

<i>Tm 2</i>	<i>NL</i>	<i>Case A</i>	<i>Case B</i>	<i>Case C</i>	<i>Case D</i>	<i>CaseA</i>	<i>CaseB</i>	<i>Case C</i>	<i>Case D</i>
					X Direction				
ChiChi HWA	-		12,0	18,5	21,0		10,0	14,0	17,0
ChiChi TCU	-		12,5	19,8	16,0		8,0	12,3	12,0
Coalinga	S		16,7	30,8	30,0		10,0	22,0	24,0
Imp Vall	-		21,0	24,0	20,0		14,0	18,0	16,0
Kobe	-		13,0	21,7	13,0		9,2	12,5	11,4
Kocaeli	-	50,4	19,5	28,5	16,0	35,8	10,0	16,0	13,7
Loma P	S-R	(RSA)	15,4	30,0	41,1	(RSA)	10,7	21,5	30,0
North	-		17,0	22,0	14,0		16,3	20,8	11,2
S Fern	S-R		12,5	27,6	44,0		8,6	21,2	13,6
Whittier	S-R		12,1	24,5	30,0		10,3	18,5	20,1
AVERAGE			15,2	24,7	24,5		10,7	17,7	16,9
MAX			21,0	30,8	44,1		16,3	22,0	30,0

Table 4 – Maximum stress (in MPa) recorded in the piping system from the time history analyses: High frequency excitations in both X- and Y- directions for all cases A-D

<i>Tm 1</i>	<i>NL</i>	<i>Case A</i>	<i>Case B</i>	<i>Case C</i>	<i>Case D</i>	<i>Case A</i>	<i>CaseB</i>	<i>Case C</i>	<i>CaseD</i>
					X Direction				
ChiChi	-		28,1	32,5	18,0		18,0	25,0	13,5
Coyotek	-		25,0	31,0	10,5		17,0	21,6	9,0
Friuli	-		16,7	28,8	22,0		14,0	20,5	18,3
Imp Vall	-		14,8	20,2	18,8		14,6	18,6	22,4
Kobe	-		22,1	32,7	24,4		19,5	25,8	19,2
Loma P	-	50,4	22,2	31,0	14,5	35,8	19,2	24,8	11,0
Managua	-	(RSA)	15,0	21,0	12,7	(RSA)	13,2	19,0	10,6
Park	-		24,0	30,0	12,0		15,0	18,0	8,0
S Fern	-		18,5	25,0	20,0		10,8	15,7	14,5
Tabas	-		12,5	16,0	12,7		9,5	12,9	9,9
AVERAGE			19,9	26,8	16,6		15,1	20,2	13,6
MAX			28,1	32,7	24,4		19,5	25,8	22,4



5. Conclusions

The seismic response of the piping system in the NPP containment building that forms part of the main cooling system of a typical reactor is studied. To this purpose, a fully 3D FEM analysis of the supporting soil, the internal structure and its mechanical equipment is carried out. The analyses include both Response Spectrum Analysis with the EC8 prescribed design spectrum, as well as Response History Analyses from actual ground motion input that is categorized in terms of the frequency content of the recorded motions as high, moderate and low. Different analysis approaches of increasing complexity (and computational cost) are carried out involving alternative considerations of soil compliance (i.e., structural fixity versus a 3D FE representation of the soil system) and geometrical nonlinearities (in terms of potential uplift and sliding along the soil-foundation interface). From all these seismic scenarios, it is evident that the assumptions made regarding the modeling of the above effects have a significant impact in the seismic demand computed within the internal piping system. It is also shown that long period pulses may result to either in uplift or sliding of the containment building if rested on soft soil formations. This, in turn, amplifies the stress demand in the pipe elbows by approximately 50-100%. Overall, Response Spectrum Analysis is proven inadequate to capture complex material and geometrically nonlinear SSI phenomena, as well as predicting the distribution of maximum stresses in the mechanical equipment.

6. References

- [1] S-H Cho, K Tanaka, J Wu, RK Robert, T Kim (2016): Effects of nuclear power plant shutdowns on electricity consumption and greenhouse gas emissions after the Tohoku Earthquake. *Energy Econ*;55:223–33.
- [2] American Society of Civil Engineers (ASCE) (1998): *Seismic Analysis of Safety-Related Nuclear Structures and Commentary*. Reston, Virginia, USA.
- [3] American Society of Civil Engineers (ASCE) (2005): *Seismic design criteria for structures, systems and components for nuclear facilities*. ASCE 43-05, Reston, Virginia, USA.
- [4] KKJ Bathe (1996): *Finite Element Procedures*. Upper Saddle River, New Jersey: Prentice Hall.
- [5] SL Kramer (1996): *Geotechnical Earthquake Engineering*. vol. 6. First. Upper Saddle River, New Jersey.
- [6] T Takada (2012) On Seismic Design Qualification of NPPs After Fukushima Event in Japan. 15th World Conf Earthq Eng., Lisbon, Portugal.
- [7] EG Bougaev, AS Gousseltsev, MO Topchiyan (1996): Seismic soil properties under reactor buildings. *Elev. World Conf. Earthq. Eng., Acapulco, Mexico*.
- [8] G Mylonakis, G Gazetas (2000): Seismic Soil-Structure Interaction: Beneficial or Detrimental? *J Earthq Eng*;4:277–301.
- [9] JL Coleman, C Bolisetti, AS Whittaker AS (2015): Time-domain soil-structure interaction analysis of nuclear facilities. *Nuclear Engineering Design*;298:264–70.
- [10] HT Hu, YH Lin (2006): Ultimate analysis of PWR prestressed concrete containment subjected to internal pressure. *Int J Press Vessel Pip*;83:161–7.
- [11] HT Hu, JL Liang (2000): Ultimate analysis of BWR Mark III reinforced concrete containment subjected to internal pressure. *Nuclear Engineering Design*;195:1–11.
- [12] C Bolisetti, AS Whittaker, HB Mason, I Almufti, M Willford (2014): Equivalent linear and nonlinear site response analysis for design and risk assessment of safety-related nuclear structures. *Nuclear Eng. Design*;275:107–21.
- [13] AJ Muzumdar, DA Meneley (2009): Large LOCA Margins in CANDU Reactors - an Overview of the COG Report. *Proc. CNS 30th Annu. Conf.*, May 31-June 3, Calgary, AB, p. 1–17.
- [14] American Society of Mechanical Engineers (ASME) (2010): *Boiler and Pressure Vessel Code Section III*.
- [15] American Society of Mechanical Engineers (ASME) (2010): *Section II, Part D: Properties (metric)*. ASME Boil Press Vessel Code 2010.
- [16] CEN (2004): *Eurocode 8: Design of structures for earthquake resistance—Part 1: General rules, seismic actions and rules for buildings (EN 1998-1: 2004)*. Eur Comm Norm Brussels 2004;1.
- [17] Y-N Huang, AS Whittaker, N Luco (2010) Seismic performance assessment of base-isolated safety-related nuclear structures. *Earthq Eng Struct Dyn*;39:1421–42.
- [18] H Lee, YC Ou, H Roh, JS Lee (2014): Simplified model and seismic response of integrated nuclear containment system based on frequency adaptive lumped-mass stick modeling approach. *KSCE J Civ Eng*.
- [19] Dassault Systèmes (2014): *Abaqus 6.14 / Analysis User's Guide*;I:862.
- [20] Atomic Energy of Canada Limited (AECL) (2004): *ACR-700 Technical Description 10810-01371-TED-001*. Revision 1. Ontario, Canada.
- [21] J Case, A Chilver, CTF Ross (1999). *Strength of Materials and Structures*. Butterworth Heinemann.